NASA Technical Memorandum 105289

Damage and Fracture in Composite Thin Shells

Levon Minnetyan
Clarkson University
Potsdam, New York

Christos C. Chamis and Pappu L.N. Murthy
Lewis Research Center
Cleveland, Ohio

Prepared for the
23rd International SAMPE Technical Conference
Lake Kiamesha, New York, October 22-24, 1991

NASA

The behavior of laminated composite structures under loading is rather complex, especially when possible degradation with preexisting damage and fracture propagation is to be considered. Internal damage in composites is often initiated as transverse cracking through one or more plies. At the presence of stress concentrations or defects, initial damage may also include fiber fracture. Further degradation is in the form of additional fiber fracture that usually leads to structural fracture. Because of the numerous possibilities with material combinations, composite geometry, ply orientations, and loading conditions, it is essential to have an effective computational capability to predict the behavior of composite structures for any loading, geometry, composite material combinations, and boundary conditions. The predictions of damage initiation, damage growth and propagation to fracture are important in evaluating the load carrying capacity and reliability of composite structures. Quantification of the structural fracture resistance is also required to evaluate the durability/life of composite structures.

The CODSTRAN (COmposite Durability STRuctural ANalysis) computer code (1) has been developed for this purpose. CODSTRAN is able to simulate damage initiation, damage growth, and fracture in composites under various loading and environmental conditions. The simulation of progressive fracture by CODSTRAN has been verified to be in reasonable agreement with experimental data from tensile tests (2). Recent additions to CODSTRAN have enabled investigation of the effects of composite degradation on structural response (3), composite damage induced by dynamic loading (4), composite structures global fracture toughness (5), and the effect of hygrothermal environment on durability (6). The objective of this paper is to describe an application of CODSTRAN to simulate damage growth and fracture progression in composite shells.

BRIEF DESCRIPTION OF CODSTRAN

CODSTRAN is an integrated, open-ended, stand alone computer code consisting of three modules: composite mechanics, finite element analysis, and damage progression modelling. The overall evaluation of composite structural durability is carried out in the damage progression module (1) that keeps track of composite degradation for the entire structure. The damage progression module relies on ICAN (7) for composite micromechanics, macromechanics and laminate analysis, and calls a finite element analysis module that uses anisotropic thick shell elements to model laminated composites (8).

Fig. 1 shows a schematic of the computational cycle in CODSTRAN. The ICAN composite mechanics module is called before and after each finite element analysis. Prior to each finite element analysis, the ICAN module computes the composite properties from the fiber

and matrix constituent characteristics and the composite layup. The laminate properties may be different at each node. The finite element analysis module accepts the composite properties that are computed by the ICAN module at each node and performs the analysis at each load increment. After an incremental finite element analysis, the computed generalized nodal force resultants and deformations are supplied to the ICAN module that evaluates the nature and amount of local damage, if any, in the plies of the composite laminate. Individual ply failure modes are determined by ICAN using failure criteria associated with the negative and positive limits of the six ply-stress components, a modified distortion energy failure criterion, and interply delamination due to relative rotation of the plies.

The generalized stress-strain relationships for each node are revised according to the composite damage evaluated by the ICAN module after each finite element analysis. The model is automatically updated with a new finite element mesh and properties, and the structure is reanalyzed for further deformation and damage. If there is no damage after a load increment, the structure is considered to be in equilibrium and an additional load increment is applied. Analysis is stopped when global structural fracture is predicted.

APPLICATION TO COMPOSITE SHELLS

A composite system made of Thornel-300 graphite fibers in an epoxy matrix (T300/Epoxy) is used to illustrate a typical CODSTRAN durability analysis. The laminate consists of fourteen 0.127 mm (0.005 in.) plies resulting in a composite shell thickness of 1.778 mm (0.07 in.). The laminate configuration is $[90_2/\pm 15/90_2/\pm 15/90_2/\mp 15/90_2]$. The 90^o plies are in the hoop direction and the $\pm 15^o$ plies are oriented with respect to the axial direction (the global y coordinate in Fig. 2a) of the shell. The cylindrical shell has a diameter of 1.016 m (40 in.) and a length of 2.032 m (80 in.). The finite element model contains 612 nodes and 576 elements as shown in Fig. 2a. At one point along the circumference, at half-length of the cylinder, initial fiber fractures in two hoop plies are prescribed. The composite shell is subjected to an internal pressure that is gradually increased until the shell is fractured. To simulate the stresses in a closed-end cylindrical pressure vessel, a uniformly distributed axial tension is applied to the cylinder such that axial stresses in the shell wall are half those developed in the hoop direction. To impose the axial loading, one of the end sections is restrained against axial translation and axial tension is applied uniformly at the opposite end of the shell. The ratio of axial load to internal pressure is kept constant at all load increments.

For a structure without defects the ICAN (7) module using linear elastic laminate theory predicts that outer hoop fibers will fracture at 3.09 MPa (448 psi) internal pressure. Linear

elastic laminate theory also predicts that, before hoop ply fracture, angle plies will experience matrix cracking at an internal pressure of 2.77 MPa (401 psi). The analysis presented in this section shows the reduction in the ultimate internal pressure because of localized damage in selected plies of the composite shell structure.

In general, overall structural damage may include individual ply damage and also through-the-thickness fracture of the composite laminate. CODSTRAN is able to simulate varied and complex composite damage mechanisms via evaluation of the individual ply failure modes and associated degradation of laminate properties. In general, the type of damage growth and the sequence of damage progression depend on the composite structure, loading, material properties, and hygrothermal conditions. A scalar damage variable, derived from the total volume of the composite material affected by the various damage mechanisms is also presented in this paper as an indicator of the level of overall damage induced by loading. This damage variable is useful for assessing the overall degradation of the given structure under the prescribed loading condition. However, it is not meant to be used to compare damages in different structures or under different loading conditions. The rate of overall damage growth with work done during composite degradation is used to evaluate the propensity of structural fracture with increasing loading. Computation of the overall damage variable has no interactive feedback on the detailed simulation of composite degradation. The procedure by which the overall damage variable is computed is given in reference (5). In this paper, the composite structure is defined to be 100 percent damaged when all plies of all nodes develop some damage. In general, global or structural fracture will occur near a defect before the 100 percent damage level is reached. Computed results will be presented up to impending global fracture.

Before the imposition of defect-induced damage on the composite shell, an internal pressure of 1.38 MPa (200 psi) is applied as the first load increment. In the absence of initial damage, ply 1 (outermost ply) longitudinal stress is 647 MPa (93.8 ksi) and ply 14 (innermost ply) longitudinal stress is 640 MPa (92.8 ksi). Ply transverse stresses in the angle plies (± 15 degrees) vary between 44.8 MPa (6.50 ksi) in ply 3 to 43.6 MPa (6.32 ksi) in ply 12.

Case I: Analysis of undamaged pressure vessel – Without imposing any initial damage, the internal pressure is gradually increased above 1.38 MPa (200 psi). CODSTRAN simulation gives a first damage initiation pressure of 2.59 MPa (376 psi). Initial damage is in the form of matrix cracking in the outer angle plies. As the pressure is further increased, matrix cracking due to excessive transverse ply stresses prevails in all angle plies of all nodes. Ply fiber fractures occur at 3.07 MPa (445 psi), resulting in structural fracture.

Case II: Cylinder with initial fiber fracture in outer surface plies – Initial damage is prescribed in the form of fiber fracture in plies 1 and 2 (the two outermost hoop plies) at one node (node 307; Fig. 2b) at an internal pressure loading of 1.38 MPa (200 psi). Table 1 shows the resulting damage progression through the thickness of the composite.

Fig. 3 shows ply 1 longitudinal stress ($\sigma_{\ell 11}$) contours immediately after plies 1 and 2 are fractured at the defective node. Ply 1 longitudinal stresses are reduced to zero at that node. Ply 2 longitudinal stresses similarly diminish to zero at the same place. A significant effect of longitudinal stress failures in plies 1 and 2 is that the shell hoop generalized membrane stresses induce local bending at the damaged node. Fig. 4 shows the displacement contours just after the prescribed defects in plies 1 and 2 have taken effect. Radial displacements at the node with prescribed damage show a significant deviation from axial symmetry. Local displacements at the damaged node are reduced significantly due to eccentricity of the hoop membrane stress resultant from the shell midsurface toward the interior of the shell. At the same time, the longitudinal stresses in plies 13 and 14 are, respectively, raised to 1.56 GPa (227 ksi) and 1.68 GPa (244 ksi), that are well above the 1.45 GPa (210 ksi) failure limit for this stress. Accordingly, CODSTRAN predicts that plies 13 and 14 are fractured subsequent to the precsribed damage in plies 1 and 2. Stresses in the remaining 10 plies remain within safe levels under the 1.38 MPa (200 psi) internal pressure. Fig. 5 shows the displacements at equilibrium after plies 13 and 14 also fracture. The deformed shape now has an outward bulge at the damaged node because of the weakening of the node after the four hoop plies fracture. Excessive deformations at the two ends of the shell, depicted in Figs. 3 and 4, are due to transition from the fixed boundary nodes to the displacements of the free interior nodes. In this study, composite structural damage is not taken into account for the two axisymmetric rows of nodes at the two ends of the shell.

To investigate further structural degradation mechanisms, the internal pressure is gradually increased. There is no further degradation of the composite structure under as high as a 2.07 MPa (300 psi) internal pressure. The next load level to cause damage growth corresponds to an internal pressure of 2.30 MPa (333 psi). On the first iteration at 2.30 MPa internal pressure, transverse ply stresses in plies 3, 4, 7, 8, and 11 are raised, respectively, to the levels of 94.5, 91.7, 91.2, 90.8, and 90.6 MPa (13.7, 13.3, 13.2, 13.2, and 13.1 ksi), all exceeding the 89.9 MPa (13.0 ksi) strength limit for $\sigma_{\ell 22T}$ computed by the ICAN module, causing transverse tensile failures in these plies. On the second iteration under the same loading, the hoop plies 6, 9, and 10 fail in ply longitudinal tension (hoop tension). Simultaneously, the remaining angle ply (ply 12) fails in transverse tension. On the third iteration, the last remaining hoop ply (ply 5) fails in tension in both longitudinal and transverse directions.

In addition, plies 13 and 14 sustain additional damage according to the Modified Distortion Energy (MDE) failure criterion. On the fourth iteration the angle plies (3, 4, 7, 8, 11, and 12) sustain additional damage due to high levels of $\sigma_{\ell 12}$ (in-plane shear) stresses. On the fifth iteration equilibrium is reached under the 2.30 MPa (333 psi) internal pressure.

When the pressure is further increased to 2.53 MPa (367 psi), nodes 306 and 308 that are adjacent to node 307 in the hoop direction (Fig. 2b) sustain damage. On the first iteration, at 2.53 MPa internal pressure, all six angle plies at node 306 and the angle plies 3, 4, 7, 8, and 11 at node 308 fail in transverse tension. On the second iteration, all hoop plies at node 306, and the hoop plies 9, 10, 13, and 14 at node 308 fail in longitudinal tension. Also, the remaining angle ply (ply 12) at node 308 fails in transverse tension. On the third iteration, all angle plies at node 306 sustain additional damage due to high levels of in-plane shear stresses. At node 308, the hoop plies 1, 2, 5, and 6 fail in both longitudinal and transverse tension. On the fourth iteration all angle plies at node 308 sustain additional damage due to high in-plane shear stresses. On the fifth iteration equilibrium is reached under the 2.53 MPa (367 psi) internal pressure as there is no additional damage.

The next level of pressure to cause additional damage is at 2.61 MPa (379 psi) that causes ply 3 to fail in transverse tension at nodes 239 and 303. Although the composite structure is able to reach equilibrium at this load, the internal pressure cannot be increased significantly above this level without causing extensive damage in the composite shell. The displacement contours at this load level are shown in Fig. 6. A significant portion of the shell is involved in the deformation pattern of the damaged region. It will be shown that this pressure level corresponds to impending structural fracture.

Case III: Initial fiber fracture in the inner surface plies – The opposite two hoop plies adjacent to the interior surface of the shell (plies 13 and 14) are prescribed to be initially damaged. The overall results are very similar to Case II. Immediately after plies 13 and 14 are assigned the prescribed damage, plies 1 and 2 fail in longitudinal tension and ply 3 fails in transverse tension. The subsequent damage progression follows the pattern of Case II.

Case IV: Initial fiber fracture in the hoop plies near mid-thickness of shell – A significantly different degradation behavior is observed if the hoop plies near the mid-surface of the shell are fractured first due to initial damage. Table 2 shows the damage progression due to initial fiber fracturing in plies 9 and 10. In this case, the prescribed damage does not cause the shell membrane stress resultant to develop a significant eccentricity, allowing the node with initial damage to resist damage propagation up to an internal pressure of 2.38 MPa (344 psi). Fig. 7 shows ply 1 longitudinal stresses at an internal pressure of 2.38 MPa that causes fracturing of ply 1. Ply 1 $\sigma_{\ell 11}$ stresses at node 307 exceed the limiting value of 1.45 GPa (210 ksi)

for the ply longitudinal stress. Because of ply damage under these stresses, CODSTRAN degrades the composite structural properties and reanalizes under the same loading. Fig. 8 shows ply 1 $\sigma_{\ell 11}$ stresses after the second iteration at the same loading. Ply 1 longitudinal stresses are diminished to zero at the damaged node because of ply fracture. Fig. 8 also indicates the stress concentration patterns along the generator of the cylindrical shell and around the hoop, emanating from the defective node. If the 2.38 MPa internal pressure is exceeded, damage growth is much more rapid, involving multiple through-the-thickness fractures resulting in the structural fracture of the shell.

Fig. 9 shows the relationship between structural damage and the applied internal pressure for Cases II and IV. In Case IV, corresponding to initial damage in plies 9 and 10, there is insignificant damage growth from 1.38 MPa (200 psi) to 2.30 MPa (333 psi) internal pressure. However, there is a rather significant amount of damage from 2.30 MPa (333 psi) to 2.38 MPa (344 psi) internal pressure. Above the 2.38 MPa internal pressure, the damage progression rate becomes even greater, as the ultimate fracture load is reached. On the other hand, in Case II, corresponding to initial damage in plies 1 and 2, local damage growth at the defective node is significant below the 2.30 MPa (333 psi) internal pressure. Yet, above the 2.30 MPa pressure, this case shows considerably greater resistance to damage propagation as compared to Case IV. The ultimate pressure for Case II is 2.61 MPa (379 psi). The ultimate pressure for Case III is the same as in Case II.

Fig. 10 shows the strain energy release rate (SERR) as a function of the internal pressure for Cases II and IV. SERR may be used as a measure of global fracture toughness of a composite structure (5). SERR is computed at structural degradation levels beginning with through-the-thickness damage growth and progressing to structural fracture. In Case II, the SERR remains sufficiently high up to an internal pressure of 2.61 MPa (379 psi), indicating substantial resistance to global fracture up to this load level. However, immediately after the 2.61 MPa pressure level is exceeded, SERR drops to a very low level, indicating negligible resistance to global fracture after this stage. In Case IV, SERR drops to a low level immediately after the prescribed damage has progressed through the thickness of the shell at 2.38 MPa (344 psi). Fig. 11 shows the SERR as a function of the induced damage. The significantly higher damage level for Case IV at the time of structural fracture indicates that in Case IV, structural damage and fracture involve a substantial portion of the composite structure rather suddenly at the onset of structural fracture.

Table 3 shows the internal pressures corresponding to first damage growth and also corresponding to ultimate structural fracture. For the shell without initial damage both linear elastic laminate theory and CODSTRAN analysis (Case I) results are given. CODSTRAN

results are given also for the shell with outer or inner surface fiber initial damage (Case II or III) and for the shell with mid-thickness fiber initial damage (Case IV). The ultimate structural fracture pressure of 3.07 MPa predicted by CODSTRAN for a composite shell without defect (Case I) is used as a reference. CODSTRAN predicts that initial damage will commence at 2.59 MPa or 84 percent of ultimate fracture loading for a defect-free shell. In case of prescribed fiber defect/damage at surface hoop plies, first damage growth starts at a pressure of 1.38 MPa (200 psi) or at 45 percent of the reference ultimate pressure, followed by structural fracture at 2.61 MPa (379 psi) or 85 percent of the reference loading. If initial fiber damage is in the hoop plies near the midsurface, first damage growth is at an internal pressure of 2.30 MPa (333 psi) or 75 percent of the reference load, followed quickly by structural fracture at 2.38 MPa (344 psi) or 77 percent of the reference load.

GENERAL REMARKS

The present investigation was limited to static pressure. CODSTRAN can be used to investigate other cases. These include: *1)* compression, *2)* bending, *3)* torsion, *4)* impact, *5)* blast pressure, *6)* fatigue, and combinations of these loads. Applications of load combinations such as vibratory fatigue loading of pressurized shells and combined impact with pressure loading due to pressurized tank drop can be investigated. The presented results are computed assuming that the composite structure is at room temperature and contains no moisture. The effects of other hygrothermal environments with higher or lower temperatures and some moisture can be included in any CODSTRAN investigation. Damage growth and fracture propagation in other types of structures such as variable thickness composites, hybrid composites, and thick composite shells can also be simulated. The relationship between composite damage and structural response properties such as natural frequencies, vibration modes, buckling loads and buckling modes can be computed by CODSTRAN for any type of structure. The durability of multi-component structures such as composite shells stiffened by space frames with flexural members can also be investigated.

SUMMARY OF RESULTS

The significant results from this investigation in which CODSTRAN (COmposite Durability STRuctural ANalysis) is used to evaluate damage growth and propagation to fracture of a thin composite shell subjected to internal pressure are as follows:

1. CODSTRAN adequately tracks the damage growth and subsequent propagation to fracture for initial defects located at the outer part, inner part, or in the mid-thickness of the shell.

2. Initial damage located in the outer part (outer surface damage) begins to grow at a lower pressure but exhibits substantial damage growth prior to shell structural fracture.

3. Initial damage located in the inner part (inner surface damage) shows an overall damage progression and fracture behavior closely similar to that of the outer surface damage.

4. Initial damage located in the mid-thickness of the shell (mid-thickness damage) requires a higher pressure to cause damage growth. However, once the damage growth pressure is reached, a sudden structural fracture stage is entered at a slightly higher pressure. This structural fracture pressure is lower than that corresponding to a surface damage.

5. Inner or outer surface fiber damage reduces the ultimate internal pressure to 85 percent of the fracture pressure of an undamaged shell. Mid-thickness fiber damage reduces the ultimate pressure to 77 percent of the undamaged shell fracture pressure. With reference to the same undamaged fracture pressure, first damage growth occurs at 45 percent pressure for surface hoop ply initial damage and at 75 percent pressure for mid-thickness hoop ply initial damage.

This paper has demonstrated that computational simulation, with the use of established composite mechanics and finite element modules, can be used to predict the effects of existing ply damage, as well as loading, on the safety and durability of composite structures.

Acknowledgment– The participation of the first author in this research was sponsored by NASA-Lewis Research Center under grant NAG-3-1101.

REFERENCES

1. C. C. Chamis and G. T. Smith, "Composite Durability Structural Analysis," NASA TM–79070, 1978.

2. T. B. Irvine and C. A. Ginty, "Progressive Fracture of Fiber Composites," *Journal of Composite Materials*, Vol. 20, March 1986, pp. 166-184.

3. L. Minnetyan, C. C. Chamis, and P. L. N. Murthy, "Structural Behavior of Composites with Progressive Fracture," NASA TM–102370, January 1990, 18 pp.

4. L. Minnetyan, P. L. N. Murthy, and C. C. Chamis, "Progression of Damage and Fracture in Composites under Dynamic Loading," NASA TM–103118, April 1990, 16 pp.

5. L. Minnetyan, P. L. N. Murthy, and C. C. Chamis, "Composite Structure Global Fracture Toughness via Computational Simulation," *Computers & Structures*, Vol. 37, No. 2, pp.175-180, 1990

6. L. Minnetyan, P. L. N. Murthy, and C. C. Chamis, "Progressive Fracture in Composites Subjected to Hygrothermal Environment," Proceedings of the 32nd SDM Conference (Part 1), Baltimore, Maryland, April 8-10, 1991, pp. 867-877.

7. P. L. N. Murthy and C. C. Chamis, *Integrated Composite Analyzer (ICAN): Users and Programmers Manual*, NASA Technical Paper 2515, March 1986.

8. S. Nakazawa, J. B. Dias, and M. S. Spiegel, *MHOST Users' Manual*, Prepared for NASA Lewis Research Center by MARC Analysis Research Corp., April 1987.

Table 1: Damage Progression Due to Initial Defect in Plies 1 and 2
Composite Shell T300/Epoxy[$90_2/\pm 15/90_2/\pm 15/90_2/\mp 15/90_2$]

Pressure (MPa)	Iteration No.	Node with Damage	Plies with New Damage	New Damage Due to
1.379	1	307	1, 2	$\sigma_{\ell 11T}$, $\sigma_{\ell 13}$
	2	307	13, 14	$\sigma_{\ell 11T}$
2.298	1	307	3,4,7,8,11	$\sigma_{\ell 22T}$, RR
	2	307	6, 9, 10	$\sigma_{\ell 11T}$
		307	12	$\sigma_{\ell 22T}$, RR
	3	307	5	$\sigma_{\ell 11T}$, $\sigma_{\ell 22T}$, MDE, RR
		307	13, 14	$\sigma_{\ell 11C}$, MDE
	4	307	3,4,7,8,11,12	$\sigma_{\ell 12}$
2.528	1	306	3,4,7,8,11,12	$\sigma_{\ell 22T}$, RR
		308	3,4,7,8,11	$\sigma_{\ell 22T}$, RR
	2	306	1,2,5,6,9,10,13,14	$\sigma_{\ell 11T}$
		308	9,10,13,14	$\sigma_{\ell 11T}$
		308	12	$\sigma_{\ell 22T}$, RR
	3	306	3,4,7,8,11,12	$\sigma_{\ell 12}$
		308	1,2,5,6	$\sigma_{\ell 11T}$, $\sigma_{\ell 22T}$, MDE
	4	307	3,4,7,8,11,12	$\sigma_{\ell 12}$
2.613	1	239	3	$\sigma_{\ell 22T}$, RR
		303	3	$\sigma_{\ell 22T}$, RR
2.625	1	239	8	$\sigma_{\ell 22T}$, RR
	2	239	12	$\sigma_{\ell 22T}$, RR
2.628	1	303	8	$\sigma_{\ell 22T}$, RR
		311	11	$\sigma_{\ell 22T}$, RR
	2	303	12	$\sigma_{\ell 22T}$, RR
		311	4, 7	$\sigma_{\ell 22T}$ (Ply 4 also RR)
	3	311	3	$\sigma_{\ell 22T}$, RR

Conversion Factor: 1 MPa = 145.04 psi

Notation: $\sigma_{\ell 11T}$ - ply longitudinal tensile stress
$\sigma_{\ell 22T}$ - ply transverse tensile stress
$\sigma_{\ell 12}$ - ply in-plane shear stress
$\sigma_{\ell 13}$ - ply longitudinal shear stress
MDE - modified distortion energy failure criterion
RR - delamination due to relative rotation

Table 2: Damage Progression Due to Initial Defect in Plies 9 and 10 Composite Shell T300/Epoxy[$90_2/\pm 15/90_2/\pm 15/90_2/\mp 15/90_2$]

Pressure (MPa)	Iteration No.	Node with Damage	Plies with New Damage	New Damage Due to
1.379	1	307	9, 10	$\sigma_{\ell 11T}$, $\sigma_{\ell 13}$
2.298	1	307	3	$\sigma_{\ell 22T}$, RR
2.375	1	274	1	$\sigma_{\ell 22T}$
		304	14	$\sigma_{\ell 22T}$
		307	1, 2	$\sigma_{\ell 11T}$
			4	$\sigma_{\ell 22T}$, RR
		310	1	$\sigma_{\ell 22T}$
	2	307	6, 13, 14	$\sigma_{\ell 11T}, MDE$
			13, 14	MDE (ply 13 also RR)
			7,8,11,12	$\sigma_{\ell 22T}$, MDE, RR
	3	307	5	$\sigma_{\ell 11T}$, $\sigma_{\ell 22T}$, MDE, RR
	4	307	3,4,7,8,11,12	$\sigma_{\ell 12}$
2.400	1	307	3,4,7,8,11,12	$\sigma_{\ell 11C}$

Conversion Factor: 1 MPa = 145.04 psi

Notation: $\sigma_{\ell 11T}$ - ply longitudinal tensile stress
$\sigma_{\ell 11T}$ - ply longitudinal tensile stress
$\sigma_{\ell 22T}$ - ply transverse tensile stress
$\sigma_{\ell 12}$ - ply in-plane shear stress
$\sigma_{\ell 13}$ - ply longitudinal shear stress
MDE - modified distortion energy failure criterion
RR - delamination due to relative rotation

Table 3: Internal Pressures at First Damage Growth and Structural Fracture Composite Shell T300/Epoxy[$90_2/\pm 15/90_2/\pm 15/90_2/\mp 15/90_2$]

	Internal Pressure (MPa)			
	Linear Elastic Laminate Theory	CODSTRAN		
		Without Initial Damage	Initial Damage in Surface Ply Fibers	Initial Damage in Mid-thickness Ply Fibers
First Damage Growth	2.765	2.590	1.379	2.298
Ultimate Structural Fracture	3.086	3.068	2.613	2.375

Conversion Factor: 1 MPa = 145.04 psi

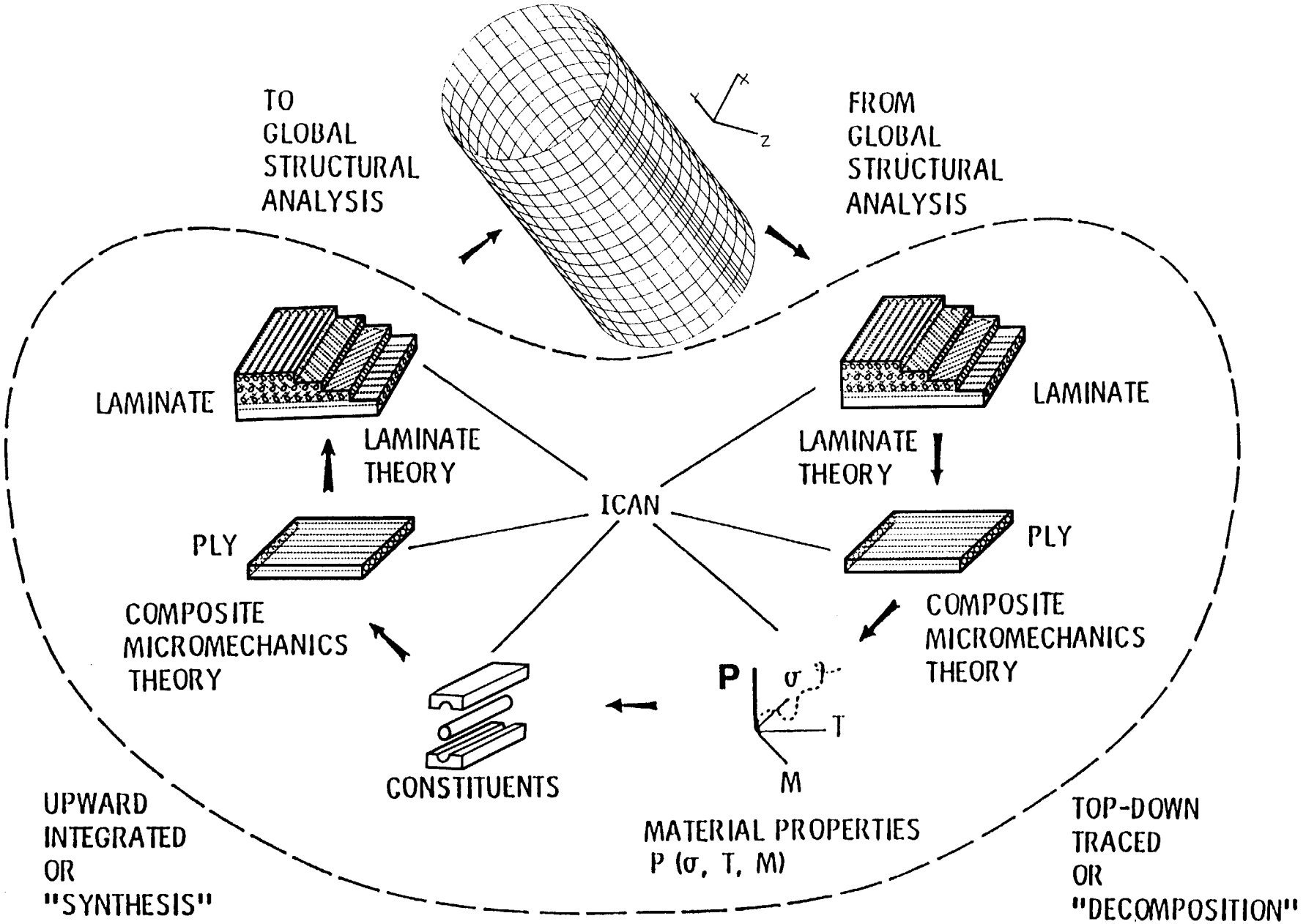

Fig. 1 Simulation of Composite Damage and Fracture Propagation via CODSTRAN

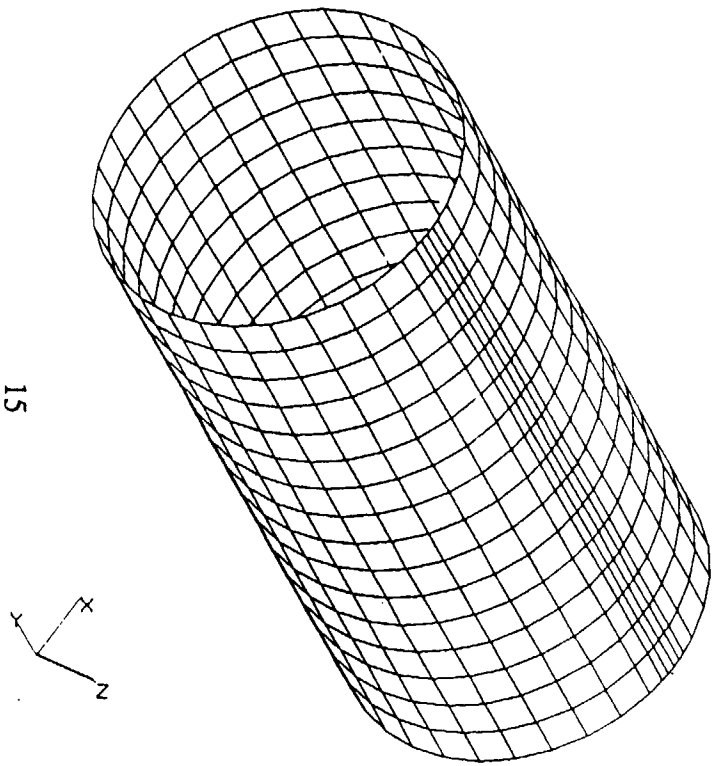

Fig. 2a Finite Element Model

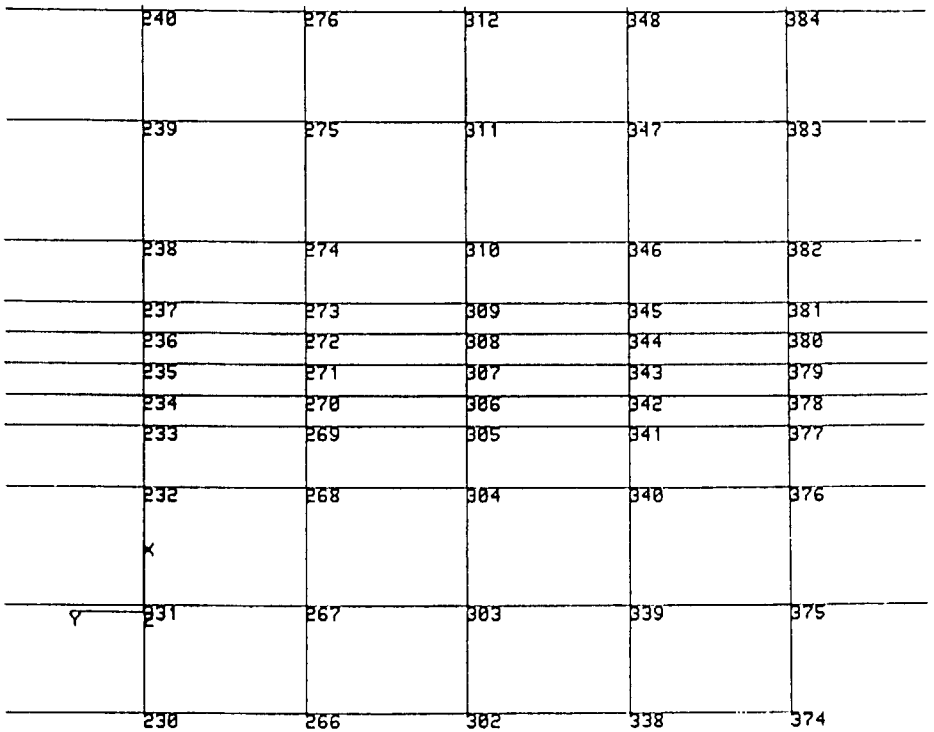

Fig. 2b Node Numbering in the Region of Initial Ply Damage

Composite Shell T300/Epoxy[$90_2/\pm15/90_2/\pm15/90_2/\mp15/90_2$]

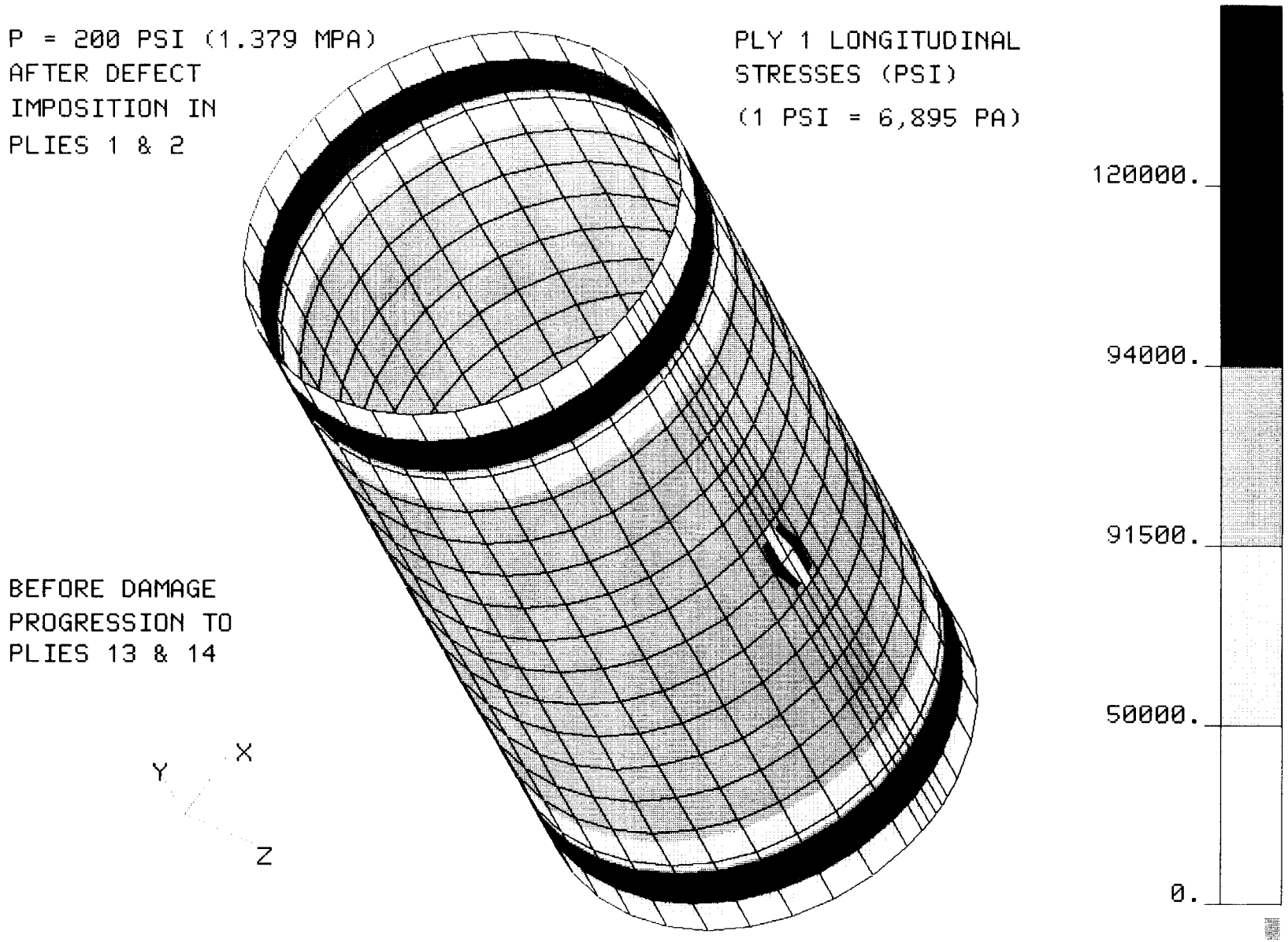

Fig. 3 Ply 1 Longitudinal Stresses after Initial Fracture of Plies 1 and 2
Composite Shell T300/Epoxy[$90_2/\pm 15/90_2/\pm 15/90_2/\mp 15/90_2$]

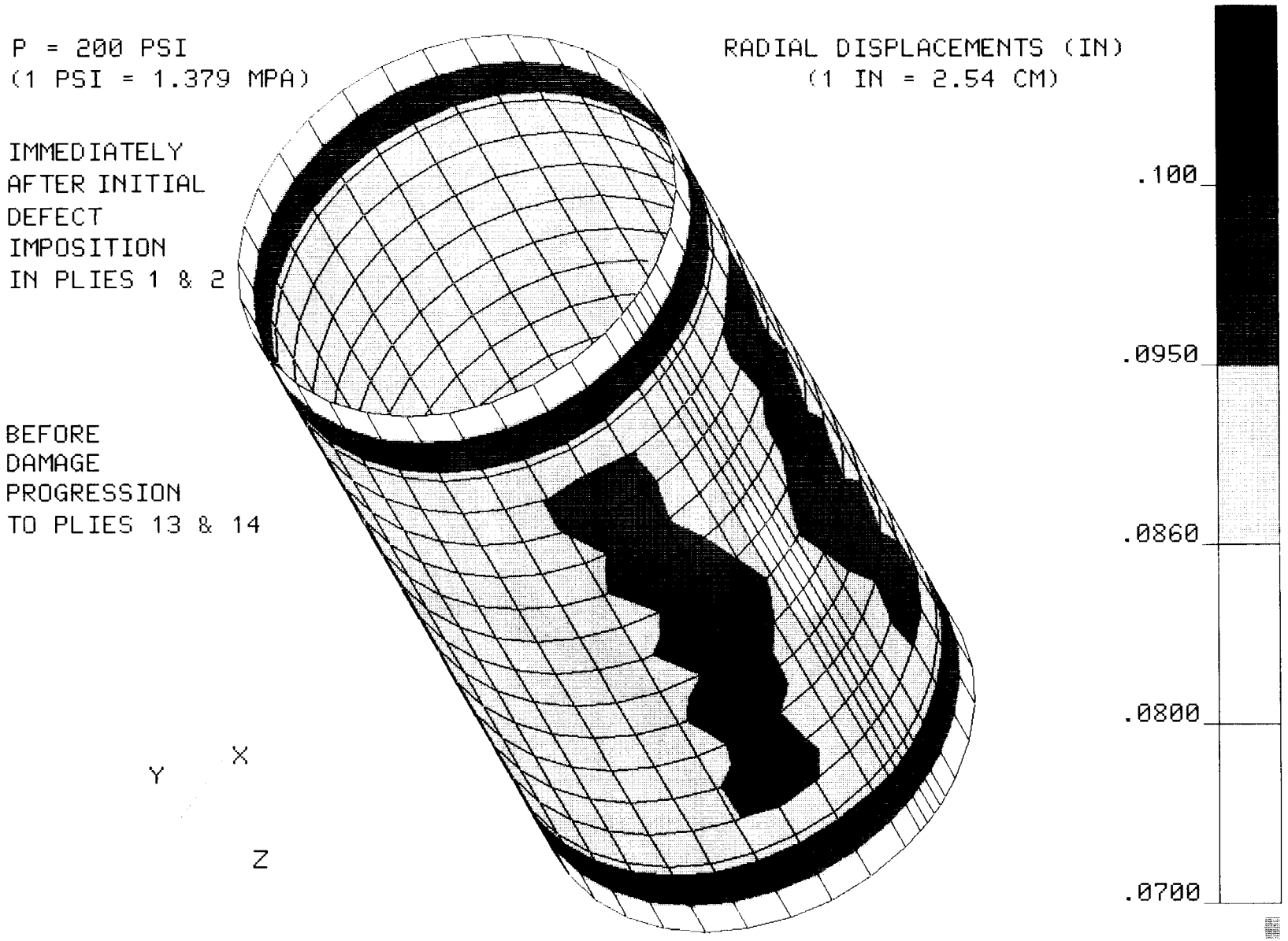

Fig. 4 Radial Displacements after Initial Fracture of Plies 1 and 2
Composite Shell T300/Epoxy[$90_2/\pm 15/90_2/\pm 15/90_2/\mp 15/90_2$]

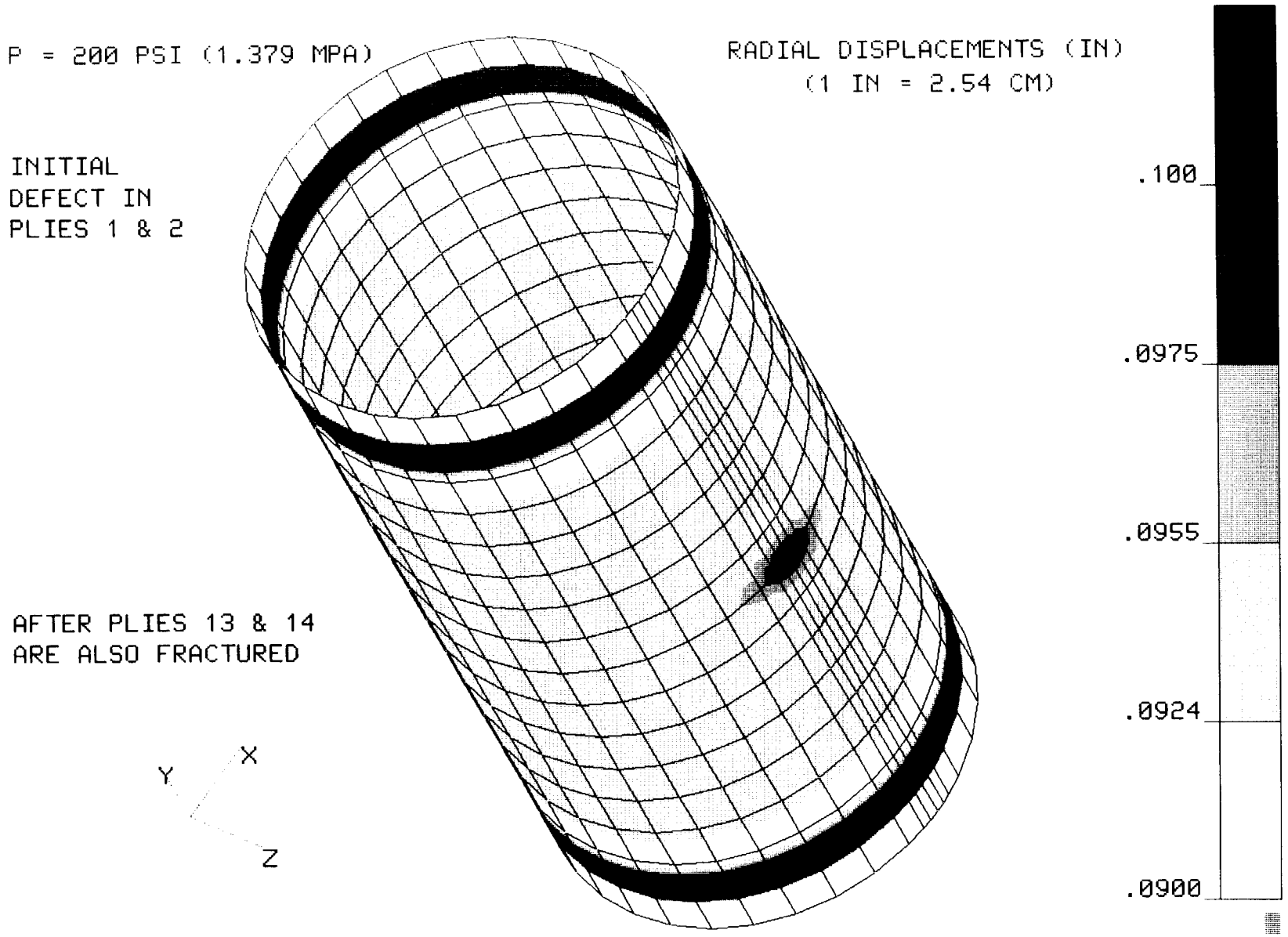

Fig. 5 Radial Displacements after Damage Progression to Plies 13 and 14
Composite Shell T300/Epoxy[$90_2/\pm 15/90_2/\pm 15/90_2/\mp 15/90_2$]

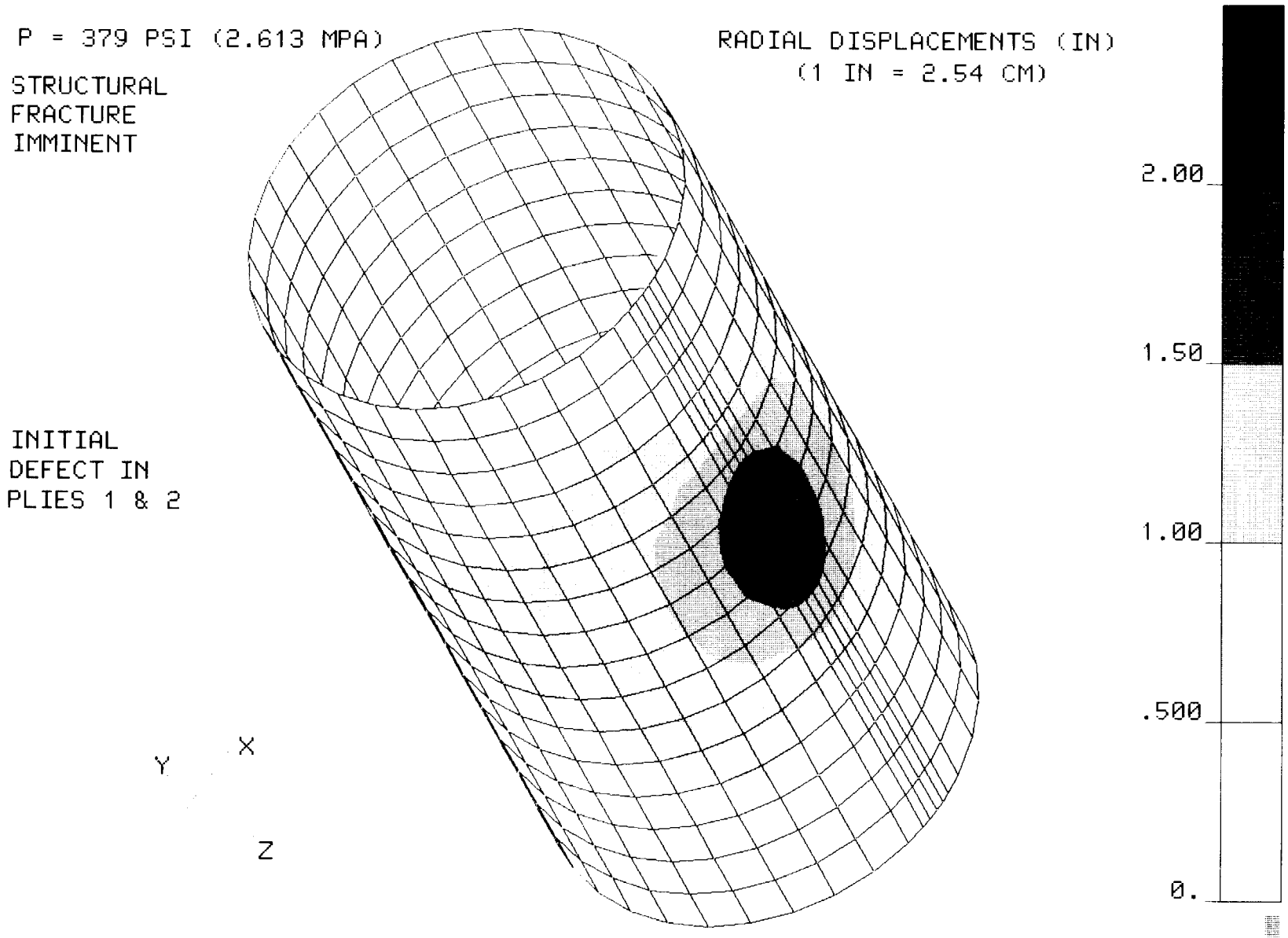

Fig. 6 Radial Displacements at 2.613 MPa (379 psi) Internal Presssure
Composite Shell T300/Epoxy[$90_2/\pm15/90_2/\pm15/90_2/\mp15/90_2$]

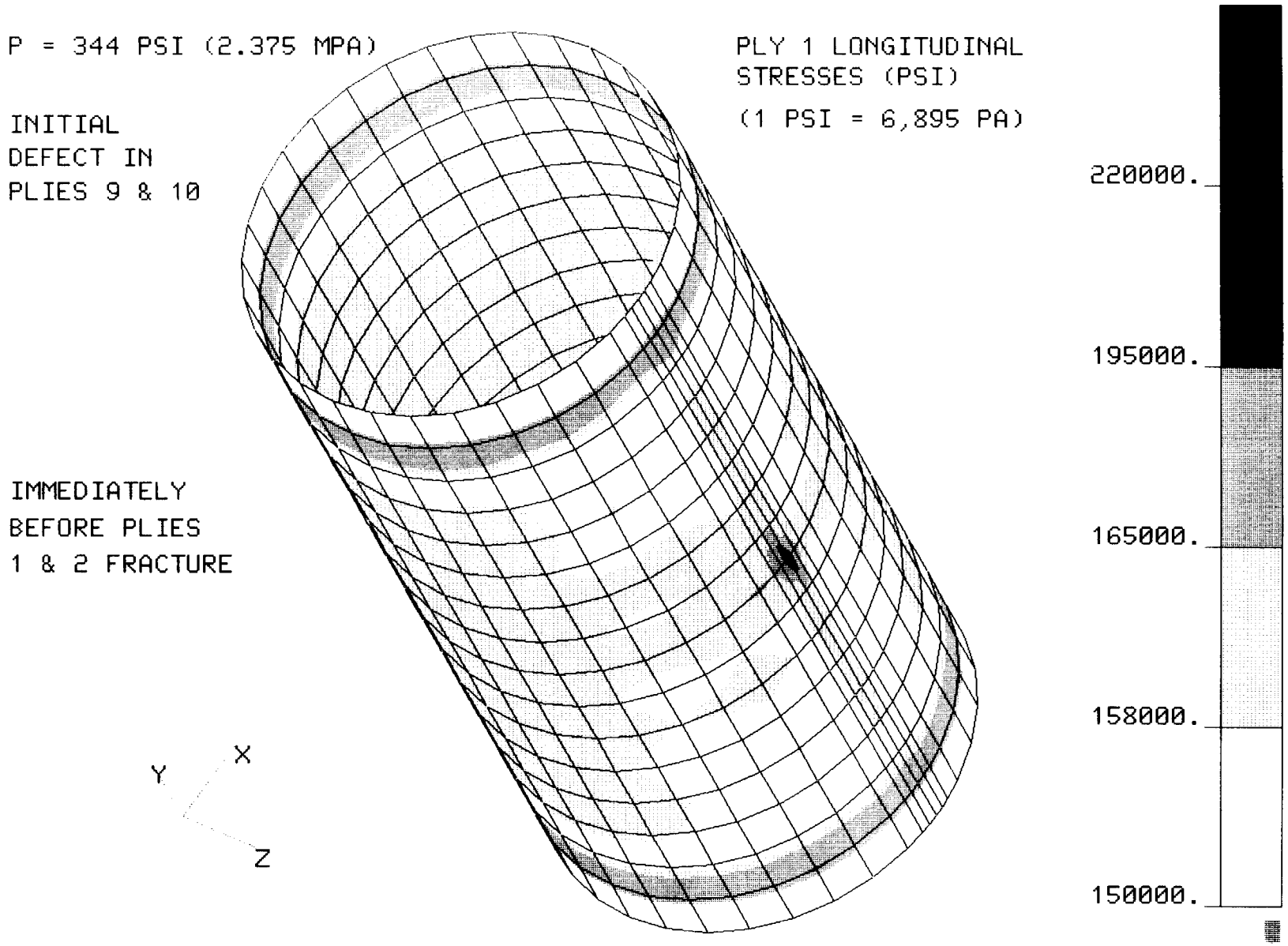

Fig. 7 Ply 1 Longitudinal Stresses at 2.375 MPa; before Ply 1 Fractures
Composite Shell T300/Epoxy[$90_2/\pm 15/90_2/\pm 15/90_2/\mp 15/90_2$]

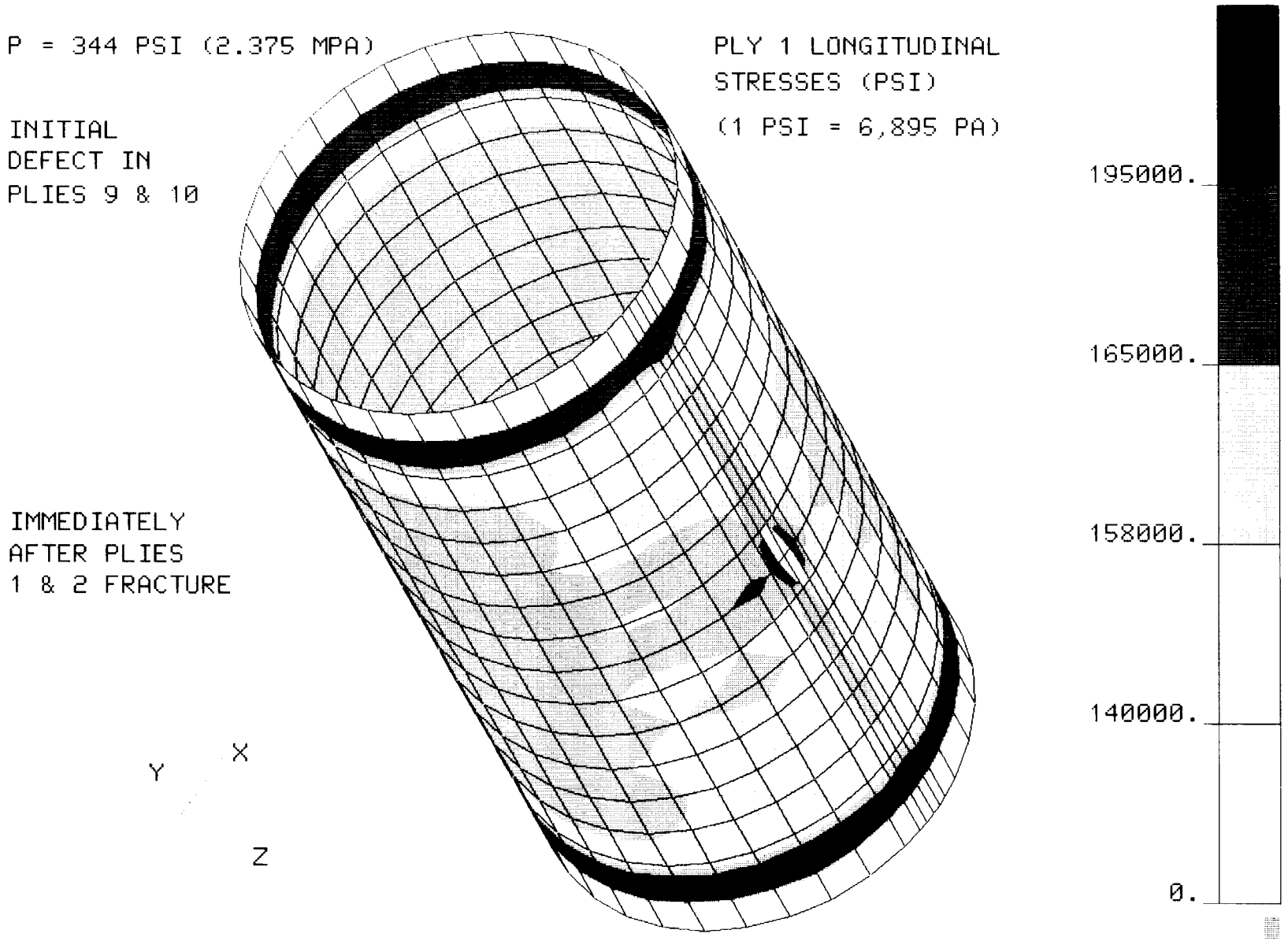

Fig. 8 Ply 1 Longitudinal Stresses at 2.375 MPa; after Ply 1 Fractures
Composite Shell T300/Epoxy[$90_2/\pm 15/90_2/\pm 15/90_2/\mp 15/90_2$]

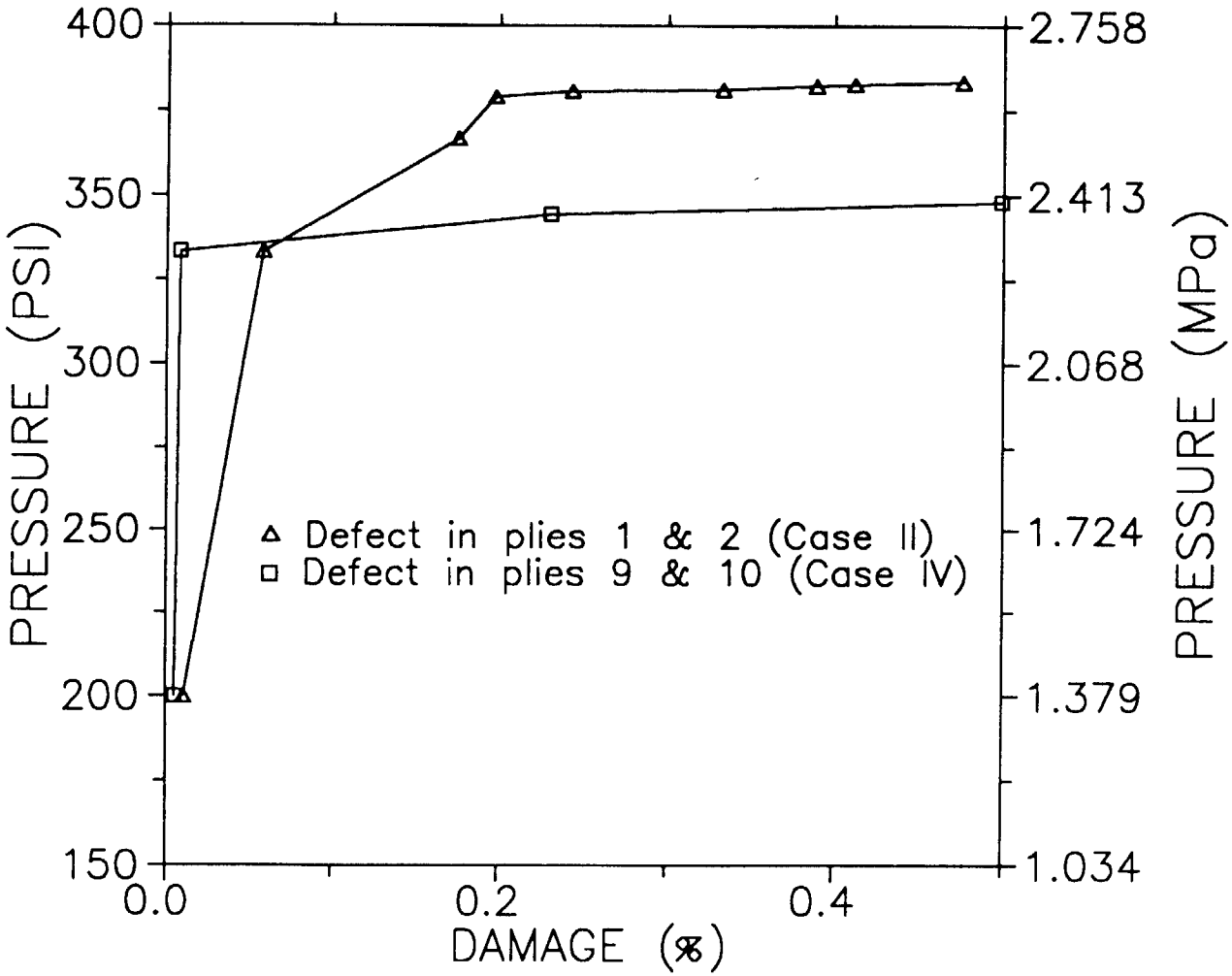

Fig. 9 Damage Propagation with Pressure
Composite Shell T300/Epoxy[$90_2/\pm15/90_2/\pm15/90_2/\mp15/90_2$]

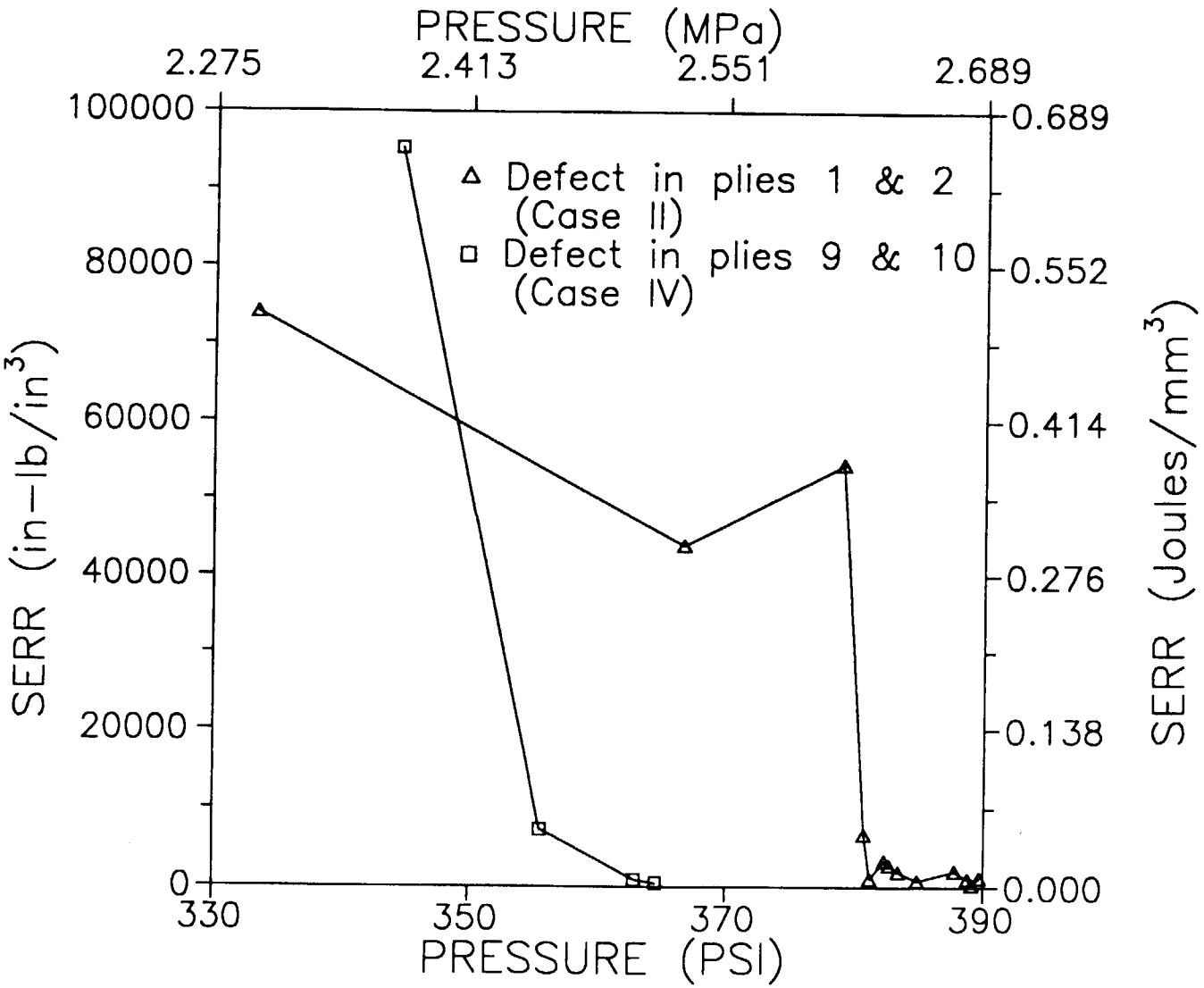

Fig. 10 Strain Energy Release Rate with Pressure
Composite Shell T300/Epoxy[$90_2/\pm15/90_2/\pm15/90_2/\mp15/90_2$]

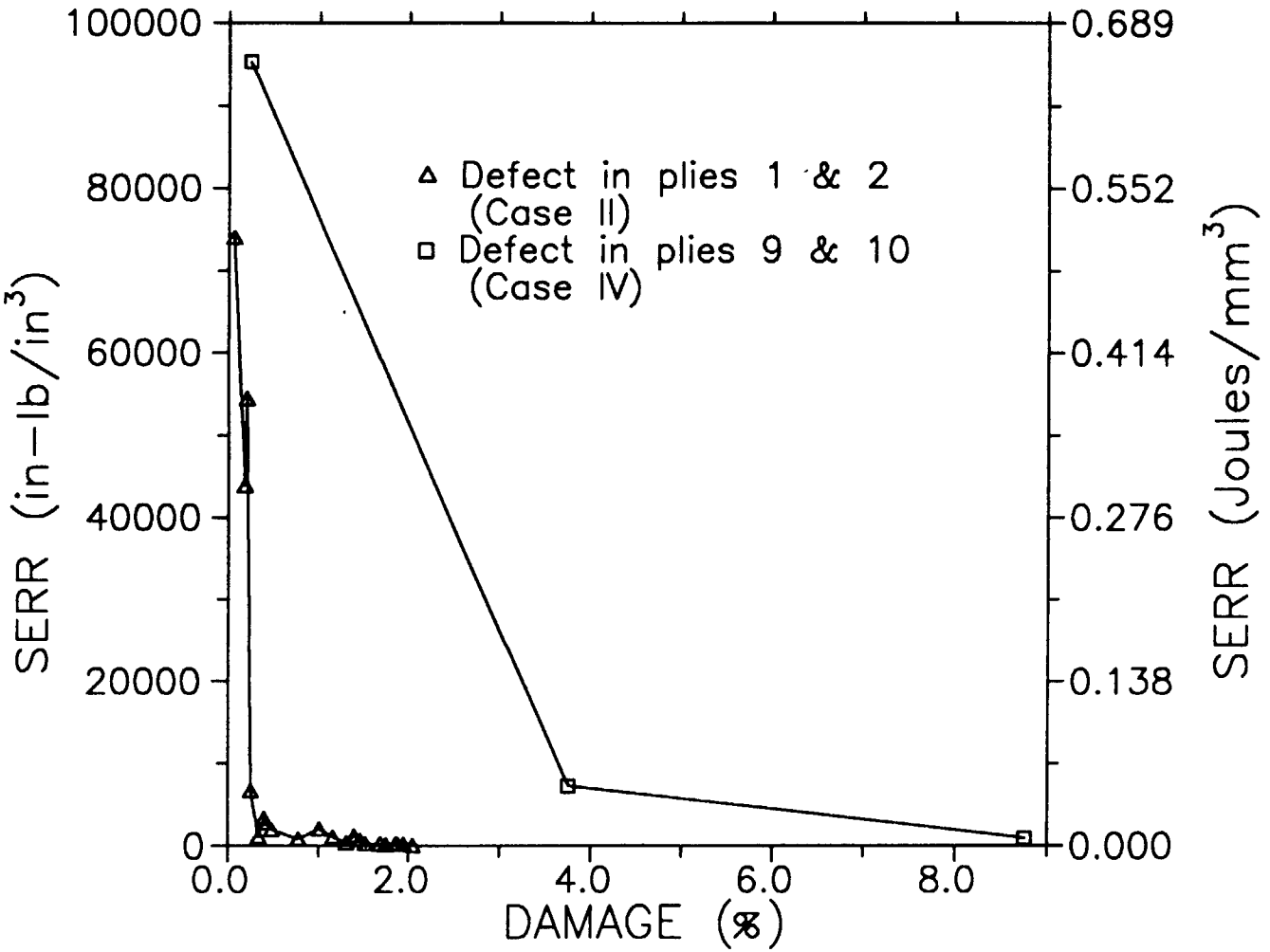

Fig. 11 Strain Energy Release Rate with Damage
Composite Shell T300/Epoxy[$90_2/\pm15/90_2/\pm15/90_2/\mp15/90_2$]

REPORT DOCUMENTATION PAGE

Form Approved
OMB No. 0704-0188

1. AGENCY USE ONLY (*Leave blank*)	2. REPORT DATE	3. REPORT TYPE AND DATES COVERED
		Technical Memorandum

4. TITLE AND SUBTITLE

Damage and Fracture in Composite Thin Shells

5. FUNDING NUMBERS

WU-505-63-5B

6. AUTHOR(S)

Levon Minnetyan, Christos C. Chamis, and Pappu L.N. Murthy

7. PERFORMING ORGANIZATION NAME(S) AND ADDRESS(ES)

National Aeronautics and Space Administration
Lewis Research Center
Cleveland, Ohio 44135-3191

8. PERFORMING ORGANIZATION REPORT NUMBER

E-6624

9. SPONSORING/MONITORING AGENCY NAMES(S) AND ADDRESS(ES)

National Aeronautics and Space Administration
Washington, D.C. 20546-0001

10. SPONSORING/MONITORING AGENCY REPORT NUMBER

NASA TM-105289

11. SUPPLEMENTARY NOTES

Prepared for the 23rd International SAMPE Technical Conference, Lake Kiamesha, New York, October 22-24, 1991. Levon Minnetyan, Clarkson University, Department of Civil and Environmental Engineering, Potsdam, New York 13699-5710. Christos C. Chamis and Pappu L.N. Murthy, NASA Lewis Research Center. Responsible person, Pappu L.N. Murthy, (216) 433-3332.

12a. DISTRIBUTION/AVAILABILITY STATEMENT

Unclassified - Unlimited
Subject Category 24

12b. DISTRIBUTION CODE

13. ABSTRACT (*Maximum 200 words*)

The effect of fiber fracture on the load carrying capability and structural behavior of a composite cylindrical shell under internal pressure is investigated. An integrated computer code is utilized for the simulation of composite structural degradation under loading. Damage initiation, damage growth, fracture progression, and global structural fracture are included in the simulation. Results demonstrate the significance of local damage on the structural durability of pressurized composite cylindrical shells.

14. SUBJECT TERMS

Composite materials; Composite structures; Computerized simulation; Damage; Degradation; Durability; Fractures (materials); Laminates; Pressure; Thinned walled shells; Structural failure

15. NUMBER OF PAGES

26

16. PRICE CODE

A03

17. SECURITY CLASSIFICATION OF REPORT	18. SECURITY CLASSIFICATION OF THIS PAGE	19. SECURITY CLASSIFICATION OF ABSTRACT	20. LIMITATION OF ABSTRACT
Unclassified	Unclassified	Unclassified	